Accepted Manuscript

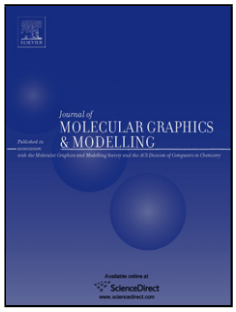

Title: Development of Efficient Docking Strategies and Structure-activity Relationship Study of the c-Met Type II Inhibitors

Authors: Ming-Jing Li, Guan-Zhao Wu, Quentin Kaas, Tao Jiang, Ri-Lei Yu

PII: S1093-3263(17)30100-6
DOI: http://dx.doi.org/doi:10.1016/j.jmgm.2017.04.004
Reference: JMG 6888

To appear in: *Journal of Molecular Graphics and Modelling*

Received date: 10-2-2017
Revised date: 5-4-2017
Accepted date: 5-4-2017

Please cite this article as: Ming-Jing Li, Guan-Zhao Wu, Quentin Kaas, Tao Jiang, Ri-Lei Yu, Development of Efficient Docking Strategies and Structure-activity Relationship Study of the c-Met Type II Inhibitors, Journal of Molecular Graphics and Modellinghttp://dx.doi.org/10.1016/j.jmgm.2017.04.004

Development of Efficient Docking Strategies and Structure-activity Relationship Study of the c-Met Type II Inhibitors

Ming-Jing Li[1†], Guan-Zhao Wu[1†], Quentin Kaas[2], Tao Jiang[1], Ri-Lei Yu[*]

[1]Key Laboratory of Marine Drugs, Chinese Ministry of Education, School of Medicine and Pharmacy, Ocean University of China, Qingdao, 266003, China

[2]Laboratory for Marine Drugs and Bioproducts of Qingdao National Laboratory for Marine Science and Technology, Qingdao 266003, China

[3]Institute for Molecular Bioscience, The University of Queensland, Brisbane, QLD, 4072 Australia

*Corresponding author. Key Laboratory of Marine Drugs, Chinese Ministry of Education, School of Medicine and Pharmacy, Ocean University of China, Qingdao, 266003, China.

Email: ryu@ouc.edu.cn

Graphical Abstract

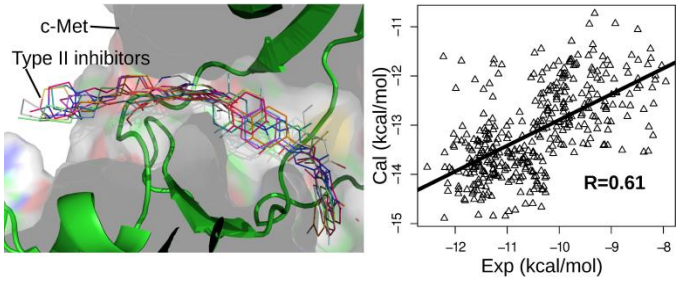

TOC

c-Met is a tyrosine kinase and an important therapeutic target for anticancer drugs. In present study, we systematically investigated the influence of a range of parameters on the correlation between experimental and calculated binding energies of type II c-Met inhibitors. Results from this study will form the basis for establishing an efficient computational docking approach for c-Met type II inhibitors design.

Highlights

• Testing a set of influences to the ranking ability of the docking program in MOE.

• Structure-activity relationship study of c-Met type II inhibitors.

• Establishing an efficient computational docking approach for c-Met type II inhibitors design.

ABSTRACT： c-Met is a transmembrane receptor tyrosine kinase and an important therapeutic target for anticancer drugs. In the present study, we systematically investigated the influence of a range of parameters on the correlation between experimental and calculated binding free energies of type II c-Met inhibitors. We especially focused on evaluating the impact of different force fields, binding energy calculation methods, docking protocols, conformation sampling strategies, and conformations of the binding site captured in several crystallographic structures. Our results suggest that the force fields, the protein flexibility, and the selected conformation of the binding site substantially influence the correlation coefficient, while the sampling strategies and ensemble docking only mildly affect the prediction accuracy. Structure-activity relationship study suggests that the structural determinants to the high binding affinity of the type II inhibitors originate from its overall linear shape, hydrophobicity, and two conserved hydrogen bonds. Results from this study will form the basis for establishing an efficient computational docking approach for c-Met type II inhibitors design.

Keywords: c-Met; docking; binding affinity; conformation; force field; computational screening

1. Introduction

c-Met is a transmembrane receptor tyrosine kinase containing an extracellular α-chain of 50 kDa, which is disulfide linked to a membrane-spanning β-chain of 145 kDa [1]. Upon binding with its high-affinity natural ligand, i.e. HGF (hepatocyte growth factor), c-Met dimerizes and each monomer undergoes the transphosphorylation of Y1234 and Y1235 in the activation loop (A-loop) in the intracellular kinase domain. The phosphorylation subsequently allows the autophosphorylation of Y1349 and Y1356 in the substrate binding site at the C-terminus [2]. The hyperactivation of c-Met often facilitates the proliferation, differentiation, and antiapoptosis of normal cells by inducing the activation of JAK/STAT [3, 4], Ras/MAPK [5, 6] and PI3K/Akt pathways [7]. An aberrant c-Met activity could therefore result in tumorigenesis, invasive growth, and cancer metastasis. HGF and/or c-Met have been implicated in a wide variety of solid tumors such as liver, breast, pancreas, lung, kidney, bladder, ovary, brain, and prostate cancers [8, 9]. Overexpression of c-Met and/or HGF is often associated with a metastatic phenotype and poor prognosis, while the activation of HGF/ c-Met signaling confers resistance to cancer therapies [9]. Therefore, c-Met is an important therapeutic target for the development of anticancer drugs.

Tremendous efforts have been devoted to the development of small-molecule c-Met inhibitors, thus leading to the identification of structurally diverse c-Met inhibitors with different binding modes [9]. Several inhibitors have been approved by FDA, among which crizotinib (Fig. 1E), which was given fast track approval in 2011 to treat patients with late-stage non-small cell lung cancer (NSCLC), and cabozantinib (Fig. 1E), which was approved for patients with medullary thyroid carcinoma (MTC) in 2012 [10]. Several drug candidates targeting c-Met have progressed into clinical trials, including INCB28060 (Phase I), tivantinib (Phase I), MK2461(Phase II),

foretinib (Phase II), BMS-777607 (Phase II), MGCD265 (Phase II), EMD 1214063 (Phase I) and golvatinib (Phase I) [10]. Because c-Met inhibitors have the potential to treat a wide range of cancers, substantial efforts are made worldwide to develop more efficient and specific inhibitors with fewer side effects and higher selectivity.

The known c-Met inhibitors in general can be classified into three classes (type I, type II and others) by virtue of their binding modes. Type I inhibitors adopt a U-shaped conformation and bind to the ATP binding site when the kinase has a 'DFG-in' conformation (Fig. 1A and B), in which the conserved DFG motif of the activation loop being in an 'in' conformation [11,32]. Crizotinib belongs to type I inhibitors that binds in an U-shaped conformation (Fig. 1A). The interactions between the R-methylbenzyloxy unit and the c-Met A-loop conformation are key to the potency of crizotinib [11]. In contrast, type II inhibitors bind to the kinase when it has a 'DFG-out' conformation, in which the conserved DFG motif of the activation loop being in an 'out' conformation [11]. These inhibitors bind to c-Met in a more extended conformation than type I inhibitors, stretching from the ATP-binding site to a deep hydrophobic pocket, as illustrated in Fig. 1C and 1D [11]. In the cocrystal structure of c-Met and foretinib, this type II inhibitor is deeply buried in the c-Met allosteric pocket with the 4-fluorophenylamine motif forcing the F1223 of the DFG motif in an inactive position. The 4-phenoxyquinoline of foretinib forms hydrogen bonds with D1222 as well as pi-pi interaction with F1223, further stabilizing the inactive conformation [12].

It has been reported that the mutation of c-Met Y1230 leads to resistance against type I inhibitors but not to type II inhibitors [11]. Type II inhibitors do not interact with the gatekeeper tyrosine residues as they bind beyond the entrance of the active sites of c-Met [13]. Type II inhibitors are therefore in general not affected mutations that disrupt the binding of type I

inhibitors. However, the majority of currently available type II c-Met inhibitors are multi-targeted inhibitors, which correlates with side effects observed during clinical trials [14]. Because of the high structural and sequential conservation of the binding sites among different kinase proteins, development of novel type II inhibitors with improved specificity remains a challenge but is also promising for overcoming mutations that defeat current antitumor drugs.

Molecular docking is a fast and efficient computational approach for determining the binding modes of c-Met type II inhibitors, and ranking their binding affinities. Accurate determination of the binding modes of these inhibitors is the first step for rational design of c-Met type II inhibitors with improved specificity. However, the accuracy of docking is limited to its capacity for dealing with the flexibility of the proteins, forcefield quality as well as conformation sampling methods.

The present study was undertaken to study the influences of different force fields, docking strategies (rigid and flexible docking), the conformation sampling methods, as well as the energy calculation methods to the docking accuracy for formulation an optimal computational docking method to predict the binding modes and affinities of c-Met type II inhibitors. And the structure-activity relationships of the c-Met type II inhibitors to c-Met were systematically investigated based on the computationally determined binding modes. The large number of c-Met inhibitors with reported activities [9,15-31] as well as the six c-Met crystal structures (pdb code: 2WGJ, 2WKM, 3ZXZ, 3ZZE, 3LQ8 and 3U6I) [11,12,14,32] in complex with some of these inhibitors gave rise to the possibility to test our methods.

2. Methords

2.1. Computational Docking

Molecular docking was performed using MOE [33]. Compounds **1** to **378, listed in supplementary table 1,** were sketched in ChemDraw and minimized in MOE. The six crystal structures of the c-Met in complex with inhibitors (pdb code: 2WGJ , 2WKM, 3ZXZ , 3ZZE, 3LQ8 and 3U6I) were retrieved from the protein data bank (http://www.rcsb.org). The binding site was assumed to be identical to that of inhibitors of the same type in the crystal structure. Both the ligand and the protein were protonated at physiological pH prior to docking. Several docking protocols, force fields and sampling methods as well as c-Met crystal structures were systematically investigated to assess their influence on the accuracy of ranking inhibitor potency.

2.2. Molecular dynamics simulations

Molecular dynamics (MD) simulations were carried out on the c-Met in complex with foretinib using the Amber 12 [34] package. Foretinib was selected as its structure is similar to the compounds we choose, which are typical type II c-Met inhibitors. GAFF and FF12SB force field were employed for the ligands and the receptor, respectively. Prior to the MD simulations, the complex was solvated into an octahedral box of TIP3P water molecules and neutralized by replacing 4 water molecules by 4 Cl^- ions. The system was minimized to remove unfavorable van der Waals interactions. The minimization consisted of two steps. First, only the water molecules and ions were minimized with 1000 steps of steepest descent minimization followed by 1000 steps of conjugate gradient minimization. Second, the restraint on the solute was removed and the whole system was relaxed with 3000 steps of steepest descent minimization and 3000 steps of conjugate gradient minimization. The cutoff of the non-bonded interactions was set to 12 Å for the energy minimization process. After minimization, MD simulation was performed. First,

the solute was restrained and the whole system was gradually heated from 10 to 300 K in 100 ps in the NVT ensemble. Then the system was equilibrated in the NPT ensemble where the temperature and pressure were kept at 300 K and 1 atm, respectively. Finally, in the production process, the whole system was unconstrained and a 50 ns molecular dynamics process was carried out. For all MD simulations the time step was set to 2 fs, the particle mesh Ewald (PME) method [35] was applied to account for long-range electrostatic interactions and the lengths of the bonds involving hydrogen atoms were fixed with the SHAKE algorithm [36].

2.3. Binding energy calculations

Binding free energy calculation and decomposition was performed using the MMGBSA script in AMBER 12 as previously described [37]. Briefly, ten frames were extracted from the last 30 ns of the MD trajectory at regular time intervals. The binding energies calculated on the ten frames were averaged.

3. Results and discussion

3.1. Influences from the force fields

The performance of nine force fields was evaluated on ranking their ability to correctly rank the binding affinities of cMet type II inhibitors. Scatter plots of the correlation between computed and experimental binding energies and for the nine force fields are shown in Fig. 2. Docking using Amber10:EHT or Amber12:EHT force field gave the best ranking of the binding affinities of these compounds, and produced a Pearson product-moment correlation coefficient (R) of 0.52, which is only slightly better than that given by the Amber99, CHARMM27, OPLS-AA or PFROSST force fields. However, application of the MMFF94, MMFF94s or MMFF94x

force fields only showed very week correlations, with R between 0.24 and 0.27. The MMFF94 was designed for modeling organic molecules, especially those of pharmaceutical interest [38], whereas the Amber force fields ff12 and ff10 were developed primarily for large proteins and nucleic acids [39]. The better performance of Amber force fields might originate from its better accuracy at modeling the dynamics of proteins. The Amber10:EHT and Amber12:EHT are recently developped force fields that combine Amber10 or Amber12 with Extended Hückel Theory (EHT) bonded parameters. When the Amber10/12EHT is applied to the docking, the Amber non-bonded model is used for all atoms, and the Amber10/12 or EHT bonded parameters are used where appropriate. Therefore, it is not surprising that application of the Amber10:EHT or Amber12:EHT force field to the docking produced a comparable correlation coefficient. To the best of our knowledge, our study is the first to systematically evaluate the influences of different force fields to the performance of computational docking.

3.2. Evaluation of the MM/GBSA rescoring

A recent computational modeling study reported that the MM/GBSA method was better at ranking small ligand binding affinities compared to docking scores [40]. MM/GBSA is an end-point method that combines molecular mechanics (MM), Generalized Born (GB) implicit solvation model and accessible surface area (SA) to estimate binding free energies [41]. This method performs well for ranking binding pose predictions based on its free-energy estimations [42]. In this study, MM/GBSA was used to re-score the binding affinities of the c-Met type II inhibitors in induced fit docking based on London dG score to further improve the correlation between the predicted binding affinities and the binding affinities derived from the experimental data. Scatter plots of the correlation between binding energies calculated using MM/GBSA method and binding energies derived from experimental data are given in Fig. 3. Rescoring the

binding affinities using MM/GBSA did not improve the binding energy ranking performance of the induced fit docking in MOE. MM/GBSA is a sensitive method, and insufficiently conformational sampling and inaccuracies in the binding poses might explain this disappointing result. The performance of London dG score is comparable to that of the MM/GBSA method.

3.3. Influence from docking methods and sampling strategies

The influence of docking protocols and energy sampling methods on binding energy predictions was evaluated. Scatter plots of the correlation of the binding energies calculated using different docking protocols and energy sampling methods versus energies derived from experimental data are given in Fig. 4. The induced fit docking protocol gave the best correlations and was distinctly better than the rigid receptor docking and virtual screening. The rigid receptor docking and virtual screening methods failed to produce any significant correlation between the calculated binding energies and the experimentally derived values, with R values of about 0.1. In contrast, binding energies calculated using induced fit method mildly correlated with experimental data, with R values around 0.4–0.5. The induced fit method was slightly improved by averaging energies of ten binding modes instead of only using the minimum energy for ranking compounds. In the induced fit docking, side chains of the residues occupying the binding site are considered flexible, which is effectively modeled using a rotamer-based library. The binding energies predicted by the induced fit method are overall lower than those computed using the rigid receptor docking and virtual screening, indicating that the fit between the ligand and receptor was better. Our results are consistent with previous studies in which flexible receptor docking gave better prediction than rigid-receptor docking [43]. Additionally, we show that combining induced fit docking with an averaging energies on several top-ranked binding modes gives optimal predictions. Averaging energies over several binding poses improve the

performance of the induced fit docking probably because several configurations help decrease the sampling bias.

3.4. Ensemble based docking

In induced-fit docking, only the flexibility of the side chains in the binding site was considered, and we will here investigate the influence of backbone conformations. To consider the flexibility of the backbone, ten frames of 50 ns MD simulations of c-Met bound to a type II inhibitor (pdb code: 3LQ8) [12] were extracted and used for ensemble docking. The correlation between the binding energies from docking using multiple frames and energies derived from experiments are shown in Fig. 5. Several methods were used to compute the energies from these docking: averaging the minimum energy of all dockings with a different frame, only recording the minimum energy resulting from docking with each of the ten frames, or averaging the top 5, 10 or 20 ranking energies from all the docking poses with all the ten frames. Fig. 5 shows that the method to compute the energy only had a minor impact on the correlation with experiments, with the averaging the top 20 ranking energies of all binding poses showing a small improvement (R=0.61) (Fig. 5E) to using a single frame docking (R=0.52) (Fig. 4D). Incorporation of backbone flexibility as sampled by MD simulations can therefore improve the performance of induced-fit docking in MOE. Previous studies have found that protein conformation sampling from MD simulations can improve the performance of virtual screening, which is consistent with our results [44-48].

3.5. Influences of the activation state of c-Met

To assess the effect of the conformation adopted by the c-Met binding site when in different activation state, docking was performed using crystal structures of c-Met bound with types I or

type II inhibitors, which bound to either the DFG-in (active) or DFG-out (inactive) states of c-Met, respectively. In the previous section, we investigated the influence of small conformational changes, which could be explored using MD simulations, whereas we here focus on larger change of conformations associated with different states of the molecular target. As shown in Fig. 6, the docking of type II inhibitors into crystal structures of c-Met bound to a type II inhibitor led to significantly better correlation with experimental binding energies than using conformation of the kinase bound to type I inhibitors. Predictions made with the DFG-in kinase conformation has nearly no correlation with experimentally-derived values, stressing that it is essential to use the appropriate activation state of the molecular target for docking. The structures of type I and type II inhibitors are noticeably different, with the former having a 'U' shape and the latter adopting a linear shape, and these difference of shapes correspond to the different steric landscapes displayed by the ATP binding pocket in the two DFG states. The c-Met structure in a DFG-out conformation, which is bound by type II inhibitors, has a narrow and deep ATP binding pocket, whereas the DFG-in conformation has a comparatively shallower binding site. Overall, results from this study showed that success of docking is highly dependent on selecting the appropriate protein activation state conformation.

3.6. Binding modes of the c-Met type II inhibitors

To give a better understanding of the structure-activity relationship of the investigated compounds, their binding modes to the c-Met are here analyzed. The binding modes of the c-Met type II inhibitors were determined by docking of these compounds to the binding site of the c-Met with DFG-out conformation using Amber10:EHT forcefield and induce fit docking. As shown in Fig. 7 A, the linear type II inhibitors are deeply embedded into a narrow binding site, and several aromatic rings form extensive interactions with hydrophobic residues of the binding

pocket (Fig. 7B), which are M1160, M1211, Y1159, I1084, A1108, L1157, F1223, F1200 and I1130. The protonated heterocyclic amine group of the inhibitors is located outside of the binding pocket (Fig. S1) where it is exposed to the solvent, suggesting its little contribution to the binding affinity. Interestingly, the models suggest that the inhibitors M1160 and D1222 establish two similar hydrogen bonds at the interface, which might explain their high affinity for c-Met (Fig. S1). The predicted binding modes of all the docked compounds are consistent with those displayed in the crystallographic structures (Fig. 7 C and D). The inhibitors bind in an extended conformation that stretches from the kinase linker to the C-helix, with the heterocyclic amine group positioned outside of the binding pocket and the aromatic ring located near the C-helix. As shown in Fig. 7C the predicted orientation of compound **378** is nearly the same to that determined using crystallography with the only difference at the fluorine substituted aromatic ring in the middle of the molecule. In contrast, the predicted conformation of the aromatic ring of compound **133** (magenta) and **242** (gray) near the C-helix is remarkably different from that determined using crystallography (blue) (PDB code: 2RFN) (Fig. 7D). These binding mode differences might originate from differences in the conformation of the C-helix region between crystal structures, as the binding mode of compounds **133** and **242** in their respective crystal structures cannot be reproduced by docking in the 3LQ8 crystal structure because the C-helix would produce steric hindrance. Thus, it is essential to select the proper crystal structure of c-Met for accurate determination of the binding mode of the ligands.

4. Conclusion

We have studied the binding affinities of a set of 378 c-Met type II inhibitors to c-Met through molecular docking in MOE. Influences of different force fields, binding energy calculation methods, docking protocols, averaging of energies on multiple poses, conformation of the

binding site of the crystal structures to the correlation coefficient between experimental and calculated binding free energies were systematically investigated, establishing an optimum computational screening approach for small compounds. Our results demonstrate the following: (i) the London dG score in MOE is sensitive to the selected force fields and the Amber10/12:EHT force field is the best for ranking the binding affinities of the compounds; (ii) the performance of the dG score in MOE is comparable to the performance of MM/GBSA; (iii) consideration of the flexibility of the binding site substantially improves the performance of docking; (iv) conformation sampling strategies only slightly affect the ability of docking for ranking the binding affinities of the compounds, and the dG docking score in MOE is not sensitive to small uncertainties in c-Met/compounds complexes; (v) using multiple frames from MD lead to a small improvement of docking predictions in MOE; (vi) the activation state of the binding site is essential to the binding affinity prediction, and the selection of the appropriate crystal structure is essential for the success of docking. To conclude, we can get the best result when we calculate the energy using Amber forcefield, induced fit docking method, and average sampling protocol on multiple frames extracted from MD, and a realtively high R value of 0.61 is reached.

The induced fit docking in MOE and other docking software does not consider the flexibility of protein backbone, and docking into alternative conformations generated using MD simulation can be used to take into account small backbone fluctuations. However, larger change of conformations, such as that of the DFG motif or activation loop associated with kinase activation status, is really challenging to predict using MD simulations. Therefore, access to a crystal structure bounds to a ligand with similar structure to the compound library to be screened is suggested to be essential for the docking.

Regarding the structure-activity relationship of the type II inhibitors studied here, their interactions with c-Met are characterized by extended interactions between hydrophobic groups and two conserved hydrogen bonds with residues in the long and narrow binding cleft. In summary, we have successfully tested a set of influences to the binding affinity ranking ability of the docking program in MOE, forming the basis for efficient computational ranking the binding affinities of c-Met type II inhibitors and determination of their binding modes. In future, it will be interesting to test the same set of influences on other kinase systems using different computational docking programs.

Acknowledgements

This work was supported by the Natural Science Foundation of China (No. 81502977); Special Foundation for Qingdao Basic Research Program (No. 15-9-1-85-jch); China Postdoctoral Science Foundation funded project (No. 861505020050); and the generous funding support from the Ocean University of China (No. 201562031 and 201512007).

Appendix A. Supplementary data

Supplementary data associated with this article can be found in the online version.

Author information

[†]These authors contribute equally to this work.

Notes

The authors declare no competing financial interest.

REFERENCES

[1] S. Giordano, C. Ponzetto, R.M. Di, C.S. Cooper, P.M. Comoglio, Tyrosine kinase receptor indistinguishable from the c-met protein, Nature. 339 (1989) 155-156.

[2] S.L. Organ, M.S. Tsao, An overview of the c-MET signaling pathway, Ther. Adv. Med. Oncol. 3 (2011) S7-S19.

[3] C. Boccaccio, M. Andò, L. Tamagnone, A. Bardelli, P. Michieli, C. Battistini, P.M. Comoglio, Induction of epithelial tubules by growth factor HGF depends on the STAT pathway, Nature. 391 (1998) 285-288.

[4] Z.A. Syed, W. Yin, K. Hughes, J.N. Gill, R. Shi, J.L. Clifford, HGF/c-met/Stat3 signaling during skin tumor cell invasion: indications for a positive feedback loop, BMC Cancer. 11 (2011) 1-11.

[5] A. Graziani, D. Gramaglia, Z.P. Dalla, P.M. Comoglio, Hepatocyte growth factor/scatter factor stimulates the Ras-guanine nucleotide exchanger, J. Biol. Chem. 268 (1993) 9165-9168.

[6] R. Paumelle, D. Tulasne, Z. Kherrouche, S. Plaza, C. Leroy, S. Reveneau, B. Vandenbunder, V. Fafeur, Hepatocyte growth factor/scatter factor activates the ETS1 transcription factor by a RAS-RAF-MEK-ERK signaling pathway, Oncogene. 21 (2002) 2309-2319.

[7] G.H. Xiao, M. Jeffers, A. Bellacosa, Y. Mitsuuchi, G.F. Vande Woude, J.R. Testa, Anti-apoptotic signaling by hepatocyte growth factor/Met via the phosphatidylinositol 3-kinase/Akt and mitogen-activated protein kinase pathways, Proc. Natl. Acad. Sci. U S A. 98 (2001) 247-252.

[8] P.C. Ma, M.S. Tretiakova, A.C. MacKinnon, N. Ramnath, C. Johnson, S. Dietrich, T. Seiwert, J.G. Christensen, R. Jagadeeswaran, T. Krausz, E.E. Vokes, A.N. Husain, R. Salgia, N. Ramnath, C. Johnson, S. Dietrich, Expression and mutational analysis of MET in human solid cancers. Genes Chromosomes Cancer, 47 (2008) 1025-1037.

[9] J.J. Cui, Targeting receptor tyrosine kinase MET in cancer: small molecule inhibitors and clinical progress, J. Med. Chem. 57 (2014) 4427-4453.

[10] https://clinicaltrials.gov/

[11] J.J. Cui, M. Tran-Dubé, H. Shen, M. Nambu, P. Kung, M. Pairish, L. Jia, J. Meng, L. Funk, I. Botrous, M. McTigue, N. Grodsky, K. Ryan, E. Padrique, G. Alton, S. Timofeevski, S. Yamazaki, Q. Li, H. Zou, J. Christensen, B. Mroczkowski, S. Bender, R.S. Kania, M.P. Edwards, Structure Based Drug Design of Crizotinib (PF-02341066), a Potent and Selective Dual Inhibitor of Mesenchymal–Epithelial Transition Factor (c-MET) Kinase and Anaplastic Lymphoma Kinase (ALK), J. Med. Chem. 54 (2011) 6342-6363.

[12] F. Qian, S. Engst, K. Yamaguchi, P. Yu, K.A. Won, L. Mock, T. Lou, J. Tan, C. Li, D. Tam, J. Lougheed, F.M. Yakes, F. Bentzien, W. Xu, T. Zaks, R. Wooster, J. Greshock, A.H. Joly, Inhibition of Tumor Cell Growth, Invasion, and Metastasis by EXEL-2880 (XL880, GSK1363089), a Novel Inhibitor of HGF and VEGF Receptor Tyrosine Kinases, Cancer. Res. 69 (2009) 8009-8016.

[13] D.W. Bowles, E.R. Kessler, A. Jimeno, Multi-targeted tyrosine kinase inhibitors in clinical development: focus on XL-184 (cabozantinib), Drugs of Today. 47 (2011) 857-868.

[14] M.H. Norman, L. Liu, M. Lee, N. Xi, I. Fellows, N.D. D'Angelo, C. Dominguez, K. Rex, S.F. Bellon, T. Kim, I. Dussault, Structure-Based Design of Novel Class II c-Met Inhibitors: 1. Identification of Pyrazolone-Based Derivatives, J. Med. Chem. 55 (2012) 1858-1867.

[15] Z. Liu, R. Wang, R. Guo, J. Hu, R. Li, Y. Zhao, P. Gong, Design, synthesis and biological evaluation of novel 6,7-disubstituted-4-phenoxyquinoline derivatives bearing 4-oxo-3,4-dihydrophthalazine-1-carboxamide moieties as c-Met kinase inhibitors, Bioorgan. Med. Chem. 22 (2014) 3642-3653.

[16] W. Liao, C. Xu, X. Ji, G. Hu, L. Ren, Y. Liu, R. Li, P. Gong, T. Sun, Design and optimization of novel 4-(2-fluorophenoxy)quinoline derivatives bearing a hydrazone moiety as c-Met kinase inhibitors, Eur. J. Med. Chem. 87 (2014) 508-518.

[17] B. Qi, B. Mi, X. Zhai, Z. Xu, X. Zhang, Z. Tian, P. Gong, Discovery and optimization of novel 4-phenoxy-6,7-disubstituted quinolines possessing semicarbazones as c-Met kinase inhibitors, Bioorgan. Med. Chem. 21 (2013) 5246-5260.

[18] Q. Tang, G. Zhang, X. Du, W. Zhu, R. Li, H. Lin, P. Li, Cheng, P. Gong, Y. Zhao, Discovery of novel 6,7-disubstituted-4-phenoxyquinoline derivatives bearing 5-(aminomethylene)pyrimidine-2,4,6-trione moiety as c-Met kinase inhibitors, Bioorgan. Med. Chem. 22 (2014) 1236-1249.

[19] Q. Tang, Y. Zhao, X. Du, L. Chong, P. Gong, C. Guo, Design, synthesis, and structure–activity relationships of novel 6,7-disubstituted-4-phenoxyquinoline derivatives as potential antitumor agents, Eur. J. Med. Chem. 69 (2013) 77-89.

[20] S. Zhou, H. Liao, C. He, Y. Dou, M. Jiang, L. Ren, Y. Zhao, P. Gong, Design, synthesis and structure–activity relationships of novel 4-phenoxyquinoline derivatives containing pyridazinone moiety as potential antitumor agents, Eur. J. Med. Chem. 83 (2014) 581-593.

[21] S. Zhou, H. Liao, M. Liu, G. Feng, B. Fu, R. Li, M. Cheng, Y. Zhao, P. Gong, Discovery andw biological

evaluation of novel 6,7-disubstituted-4-(2-fluorophenoxy)quinoline derivatives possessing 1,2,3-triazole-4-carboxamide moiety as c-Met kinase inhibitors, Bioorgan. Med. Chem. 22 (2014) 6438-6452.
[22] W. Liao, G. Hu, Z. Guo, D. Sun, L. Zhang, Y. Bu, Y. Li, Y. Liu, P. Gong, Design and biological evaluation of novel 4-(2-fluorophenoxy)quinoline derivatives bearing an imidazolone moiety as c-Met kinase inhibitors, Bioorgan. Med. Chem. 23 (2015) 4410-4422.
[23] X. Jiang, H. Liu, Z. Song, X. Peng, Y. Ji, Q. Yao, M. Ai, Geng, A. Zhang, Discovery and SAR study of c-Met kinase inhibitors bearing an 3-amino-benzo[d]isoxazole or 3-aminoindazole scaffold, Bioorgan. Med. Chem. 23 (2015) 564-578.
[24] N. She, L. Zhuo, W. Jiang, X. Zhu, J. Wang, Z. Ming, X. Zhao, X. Cong, W. Huang, Design, synthesis and evaluation of highly selective pyridone-based class II MET inhibitors, Bioorg. Med. Chem. Lett. 24 (2014) 3351-3355.
[25] S. Claridge, F. Raeppel, M. Granger, N. Bernstein, O. Saavedra, L. Zhan, D. Llewellyn, A. Wahhab, R. Deziel, J. Rahil, N. Beaulieu, H. Nguyen, I. Dupont, A. Barsalou, C. Beaulieu, I. Chute, S. Gravel, M. Robert, S. Lefebvre, M. Dubay, R. Pascal, J. Gillespie, Z. Jin, J. Wang, J.M. Besterman, A.R. MacLeod, A. Vaisburg, Discovery of a novel and potent series of thieno[3,2-b]pyridine-based inhibitors of c-Met and VEGFR2 tyrosine kinases, Bioorg. Med. Chem. Lett. 18 (2008) 2793-2798.
[26] M. Mannion, S. Raeppel, S. Claridge, N. Zhou, O. Saavedra, L. Isakovic, L.Zhan, F. Gaudette, F. Raeppel, R. Déziel, N. Beaulieu, H. Nguyen, I. Chute, C. Beaulieu, I. Dupont, M. Robert, S. Lefebvre, M. Dubay, J. Rahil, J. Wang, H. Ste-Croix, A. Robert Macleod, J.M. Besterman, A. Vaisburg,N-(4-(6,7-Disubstituted-quinolin-4-yloxy)-3-fluorophenyl)-2-oxo-3-phenylimidazolidine-1-carboxamides: A novel series of dual c-Met/VEGFR2 receptor tyrosine kinase inhibitors, Bioorg. Med. Chem. Lett. 19 (2009) 6552-6556.
[27] G.M. Schroeder, X. Chen, D.K. Williams, D.S. Nirschl, Z. Cai, D. Wei, J.S. Tokarski, Y. An, J. Sack, Z. Chen, T. Huynh, W. Vaccaro, M. Poss, B. Wautlet, J. Gullo-Brown, K. Kellar, V. Manne, J.T. Hunt, T.W. Wong, L.J. Lombardo, J. Fargnoli, R.M. Borzilleri, Identification of pyrrolo[2,1-f][1,2,4]triazine-based inhibitors of Met kinase, Bioorg. Med. Chem. Lett. 18 (2008) 1945-1951.
[28] Z. Zhan, J. Ai, Q. Liu, Y. Ji, T. Chen, Y. Xu, M. Geng, W. Duan, Discovery of Anilinopyrimidines as Dual Inhibitors of c-Met and VEGFR-2: Synthesis, SAR, and Cellular Activity, ACS Med. Chem. Lett. 5 (2014) 673-678.
[29] S. Li, Q. Huang, Y. Liu, X. Zhang, S. Liu, C. He, P. Gong, Design, synthesis and antitumour activity of bisquinoline derivatives connected by 4-oxy-3-fluoroaniline moiety, Eur. J. Med. Chem. 64 (2013) 62-73.
[30] S. Li, Y. Zhao, K. Wang, Y. Gao, J. Han, B. Cui, P. Gong, Discovery of novel 4-(2-fluorophenoxy)quinoline derivatives bearing 4-oxo-1,4-dihydrocinnoline-3-carboxamide moiety as c-Met kinase inhibitors, Bioorgan. Med. Chem. 21 (2013) 2843-2855.
[31] O. Saavedra, S. Claridge, L. Zhan, F. Raeppel, M.C. Granger, S. Raeppel, M. Mannion, F. Gaudette, N. Zhou, L. Isakovic, N. Bernstein, R. Déziel, H. Nguyen, N. Beaulieu, C. Beaulieu, I. Dupont, J. Wang, A.R. Macleod, J.M. Besterman, A. Vaisburg, (2009). N 3-Arylmalonamides: A new series of thieno [3, 2-b] pyridine based inhibitors of c-Met and VEGFR2 tyrosine kinases, Bioorg. Med. Chem. Lett. 19.24 (2009) 6836-6839.
[32] J.J. Cui, M. McTigue, M. Nambu, M. Tran-Dubé, M. Pairish, H. Shen, L. Jia, H. Cheng, J. Hoffman, P. Le, M. Jalaie, G.H. Goetz, M. Koenig, T. Vojkovsky, F. Zhang, S. Do, I. Botrous, K. Ryan, N. Grodsky, Y. Deng, M. Parker, S. Timofeevski, B.W. Murray, S. Yamazaki, S. Aguirre, Q. Li, H. Zou, J. Christensen, Correction to Discovery of a Novel Class of Exquisitely Selective Mesenchymal-Epithelial Transition Factor (c-MET) Protein Kinase Inhibitors and Identification of the Clinical Candidate 2-(4-(1-(Quinolin-6-ylmethyl)-1H-[1,2,3]triazolo[4,5-b]pyrazin-6-yl)-1H-pyrazol-1-yl)ethanol (PF-04217903) for the Treatment of Cancer, J. Med. Chem. 55 (2012) 8091−8109.
[44] S. Vilar, G. Cozza, S. Moro, Medicinal chemistry and the molecular operating environment (MOE): application of QSAR and molecular docking to drug discovery, Curr. Top. Med. Chem. 8 (2008) 1555-1572.
[45] T. Steinbrecher, J. Latzer, D.A. Case, Revised AMBER Parameters for Bioorganic Phosphates, J. Chem. Theory. Comput. 8 (2012) 4405-4412.
[46] T. Darden, D. York, L. Pedersen, Particle mesh Ewald: An N·log(N) method for Ewald sums in large systems, J. Chem. Phys. 98 (1993) 10089-10092.
[47] J.P. Ryckaert, G. Ciccotti, H.J.C. Berendsen, Numerical integration of the cartesian equations of motion of a system with constraints: molecular dynamics of n -alkanes, J. Comput. Phys. 23 (1997) 292-301.
[48] R. Yu, D.J. Craik, Q. Kaas, Blockade of neuronal α7-nAChR by α-conotoxin ImI explained by computational scanning and energy calculations, PLoS. Comput. Biol. 7 (2011) e1002011.
[33] T.A. Halgren, MMFF VI. MMFF94s option for energy minimization studies, J. Comput. Chem. 20 (1999) 720-729.
[34] S.J. Weiner, P.A. Kollman, D.T. Nguyen, D.A. Case, An all atom force field for simulations of proteins and nucleic acids, J. Comput. Chem. 7 (1986) 230-252.

[35] H. Sun, Y. Li, M. Shen, S. Tian, L. Xu, P. Pan, Y. Guan, T. Hou, Assessing the performance of MM/PBSA and MM/GBSA methods. 5. Improved docking performance using high solute dielectric constant MM/GBSA and MM/PBSA rescoring, Phys. Chem. Chem. Phys.16 (2014) 22035-22045.
[36] J. Wang, P. Morin, W. Wang, P.A. Kollman, Use of MM-PBSA in reproducing the binding free energies to HI-1 RT of TIBO derivatives and predicting the binding mode to HIV-1 RT of efavirenz by docking and MM-PBSA, J. Am. Chem. Soc. 123 (2001) 5221–5230.
[37] T. Hou, J. Wang, Y. Li, W. Wang, Assessing the performance of the molecular mechanics/Poisson Boltzmann surface area and molecular mechanics/generalized Born surface area methods. II. The accuracy of ranking poses generated from docking, J. Comput. Chem. 32 (2011) 866-877.
[38] W. Sherman, T. Day, M.P. Jacobson, R.A. Friesner, R. Farid, Novel procedure for modeling ligand/receptor induced fit effects, J. Med. Chem. 49 (2006) 534-553.
[39] Á. Tarcsay, G. Paragi, M. Vass, B. Jójárt, F. Bogár, G.M. Keserű, The Impact of Molecular Dynamics Sampling on the Performance of Virtual Screening against GPCRs, J. Chem. Inf. Model. 53 (2013) 2990-2999.
[40] A. Dixit, G.M. Verkhivker, Integrating Ligand-Based and Protein-Centric Virtual Screening of Kinase Inhibitors Using Ensembles of Multiple Protein Kinase Genes and Conformations, J. Chem. Inf. Model. 52 (2012) 2501-2515.
[41] D. Bajusz, G.G. Ferenczy, G.M. Keseru, Discovery of Subtype Selective Janus Kinase (JAK) Inhibitors by Structure-Based Virtual Screening, J. Chem. Inf. Model. 56 (2016) 234-247.
[42] A.J. Campbell, M.L. Lamb, D. Josephmccarthy, Joseph-McCarthy, Ensemble-Based Docking Using Biased Molecular Dynamics, J. Chem. Inf. Model. 54 (2014) 2127-2138.
[43] E.M. Novoa, L.R.D. Pouplana, X. Barril, M. Orozco, Ensemble Docking from Homology Models, J. Chem. Theory Comput. 6 (2010) 2547-2557.

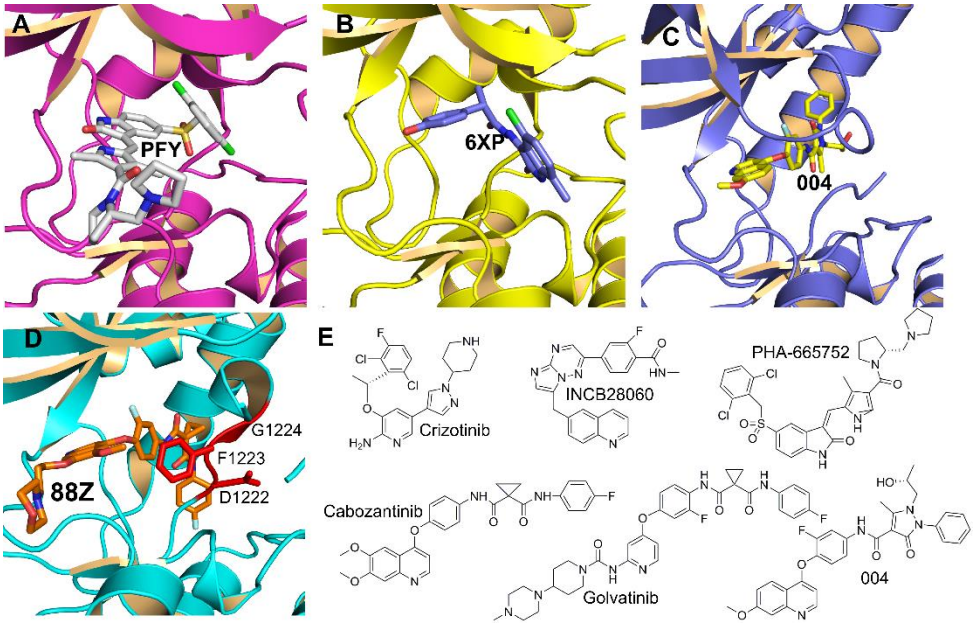

Fig. 1. Crystal structures of complexes between c-Met and some of its inhibitors. A) (pdb code: 2WKM) and B) (pdb code: 3ZZE) binding mode of type I inhibitors Pf-02341066 and Pf-04217903. C) (pdb code:3U6I) and D) (pdb code: 3LQ8) binding mode of type II c-Met inhibitors. E) structure of several c-Met type I inhibitors (Crizotinib, INCB28060, PHA-665752) and c-Met type II inhibitors (Cabozantinib, Golvatinib). The DFG motif was shown in red color in D.

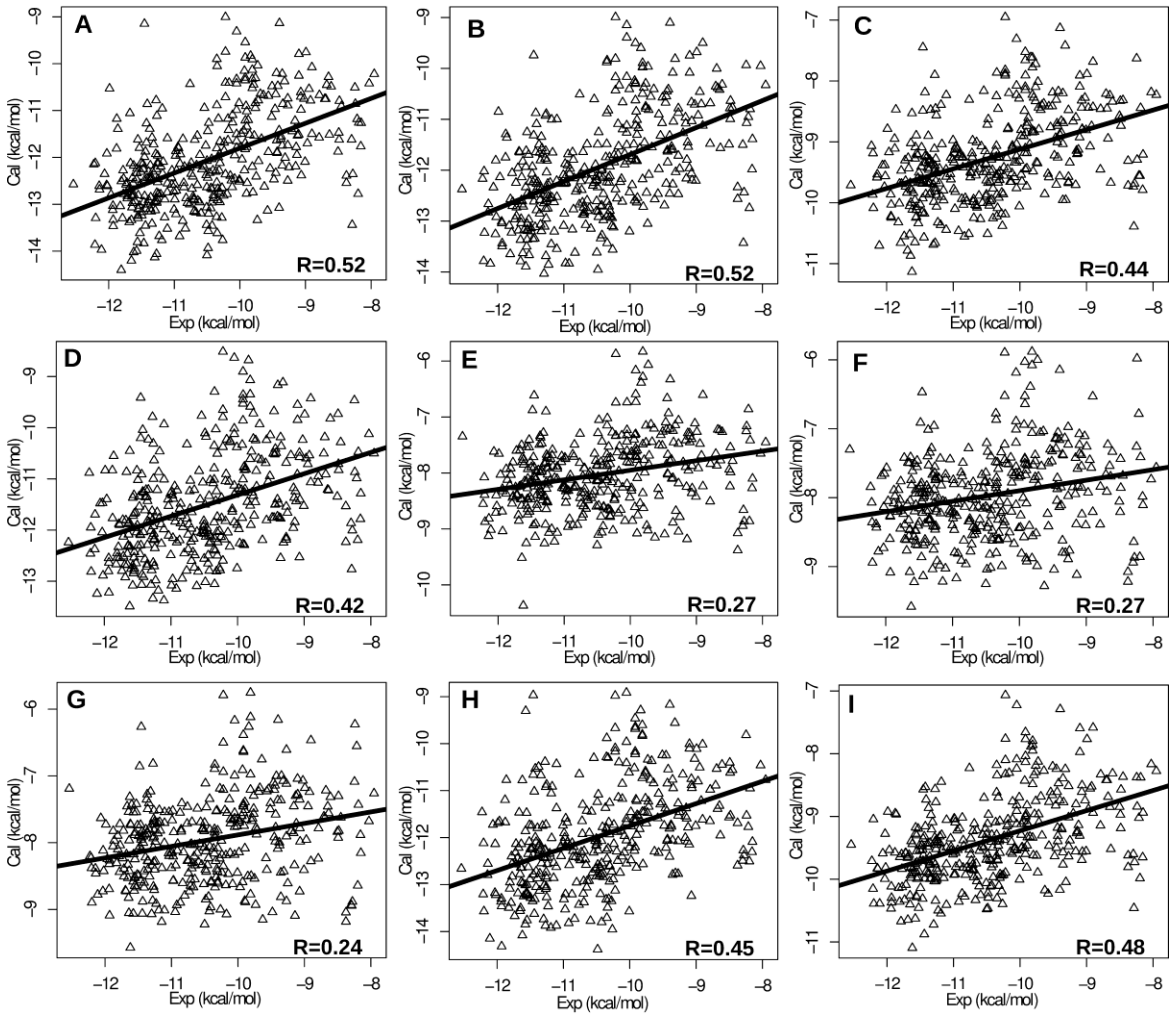

Fig. 2. Influences of the force fields to the correlation between the binding energies from docking (y-axis) and from experiment (x-axis). The binding energies of the compounds were calculated using different force fields: Amber12:EHT (A), Amber10:EHT (B), Amber99 (C), CHARMM27 (D), MMFF94 (E), MMFF94s (F), MMFF94x (G), OPLS-AA (H), and PFROSST (I). For each force field, 378 compounds were docked into the binding site of the crystal structure of c-Met (pdb code: 3LQ8) and averaged energy sampling method. The experimental binding energies were derived from several studies [9,15-31].

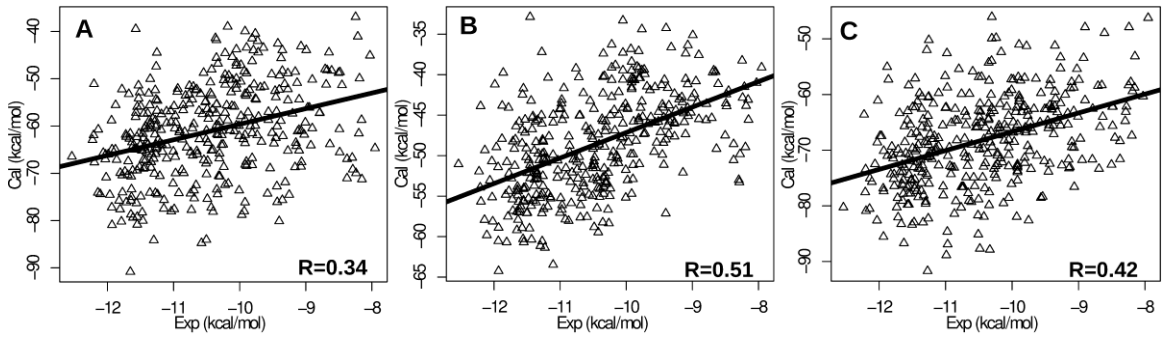

Fig. 3. Correlations between binding energies calculated using MM/GBSA method and binding energies derived from experimental data. A) Binding energies calculated using only the top ranked binding mode resulting from a docking in a crystal structure of c-Met (pdb code: 3LQ8); B) Binding energies calculated as the average binding energies between the top 10 binding modes resulting from docking in a crystal structure of c-Met (pdb code: 3LQ8); C) Binding energies of the best scored binding mode among 10 frames extracted from MD.

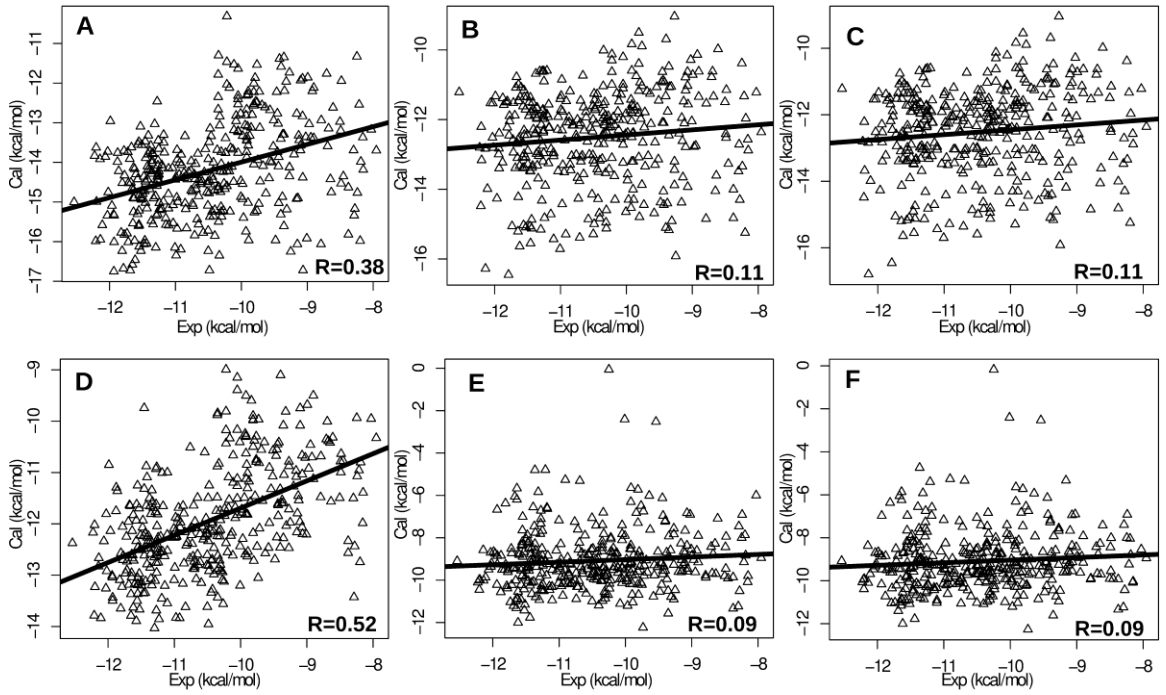

Fig. 4. Influences of the docking protocols and energy sampling methods to the correlation between experimentally derived (x-axis) and computationally calculated (y-axis) binding energies. A)–F), the binding energies were calculated using different docking protocols, including induced fit (A,D), rigid receptor (B,E), and virtual screening (C,F). The binding energies of the

docked ligands were computed two strategies, either as the minimum energy (A-C) or as the average energy (D-F) from 10 binding modes generated by docking. The 378 compounds were docked into the binding site of the crystal structure of c-Met (pdb code: 3LQ8) using the Amber10:EHT force field**.**

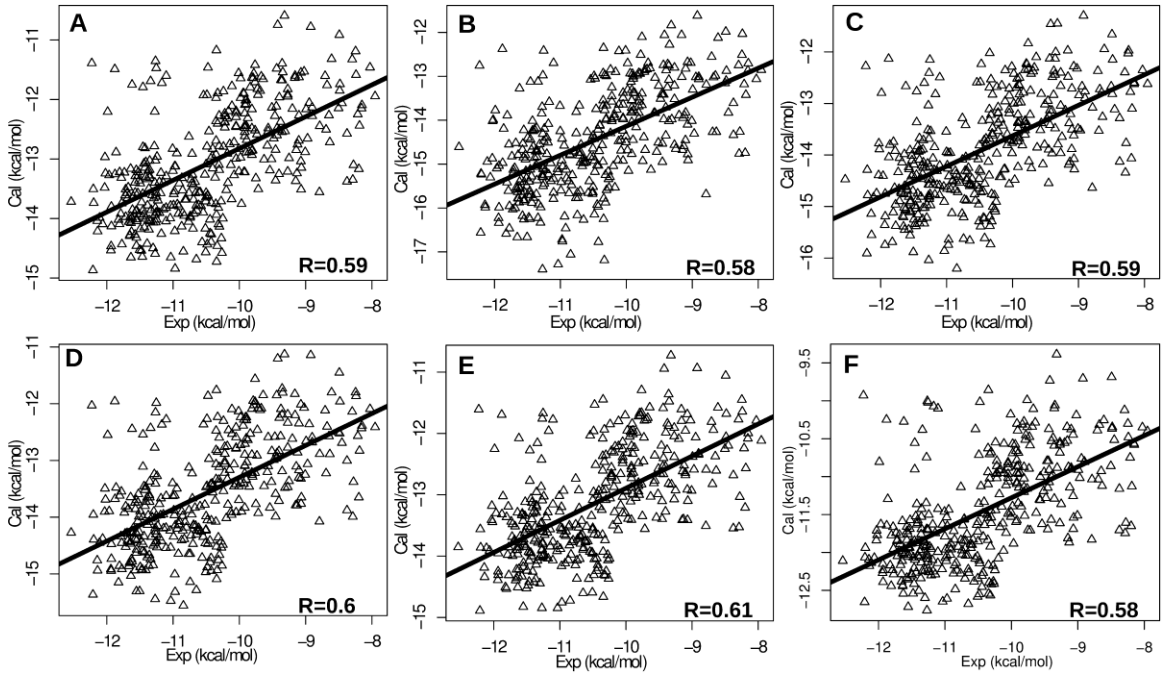

Fig. 5. Correlation between the binding energies derived from experiment (x-axis) and binding energies calculated from multi-frame based docking (y-axis). The 378 compounds were docked into ten conformations of the c-Met binding site extracted from a 50 ns MD simulation. The binding energies were computed as A) the average of the minimum binding energies obtained in each of the ten conformations, or B) the minimum binding energy whatever the binding site conformation, or C) the average of the 5 minimum energies whatever the binding site conformation; or D) the average of the 10 minimum energies whatever the binding site conformation, or E) the average of the 20 minimum energies whatever the binding site conformation, or F) the average energy for all the binding poses whatever the binding site conformation. The 10 frames were evenly extracted from the 50 ns MD simulation of the crystal structure of c-Met in complex with type II inhibitor (pdb code: 3LQ8).

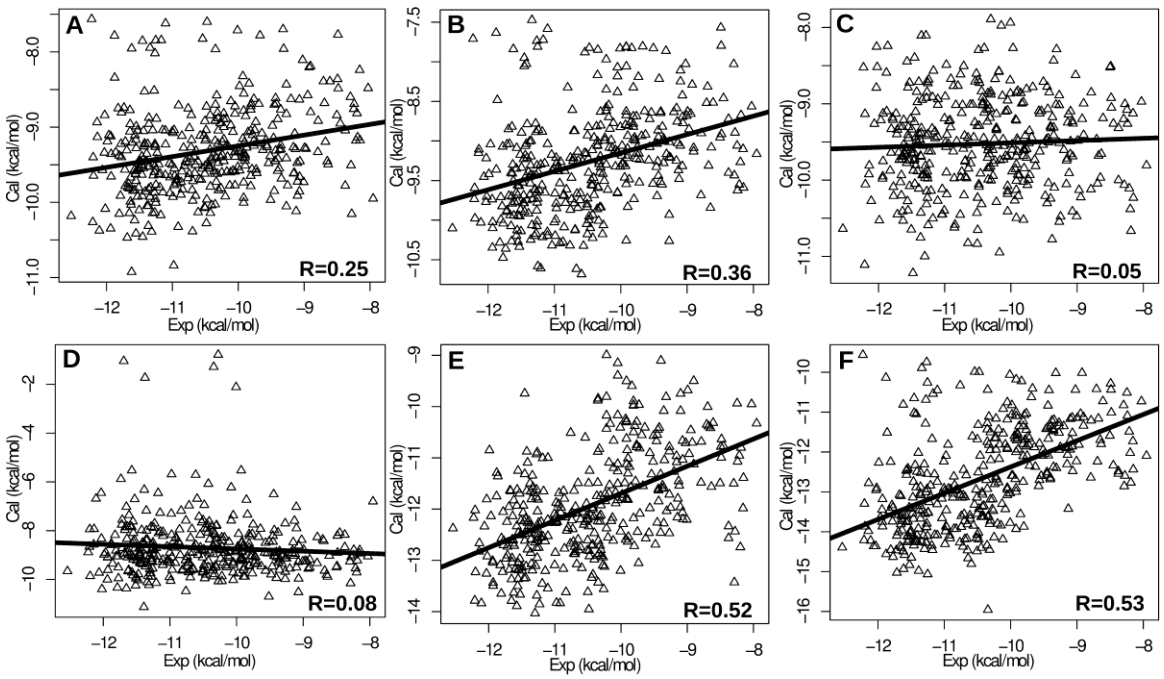

Fig. 6. Influence of the activate state of c-Met to the correlation between binding energies calculated from docking (y-axis) and binding energies derived from experiment (x-axis). The conformation of c-Met in six crystal structures of complexes between c-Met and either type I (panels A, B, C and D) or type II (panels E, and F) inhibitors were used for docking. The type I inhibitors bind to the activated, DFG-in state of the kinase, whereas the type II inhibitors bind to the inactivated, DFG-out state of the kinase. A) to F) correspond to pdb codes 2WGJ, 2WKM, 3ZXZ 3ZZE, 3LQ8 and 3U6I, respectively.

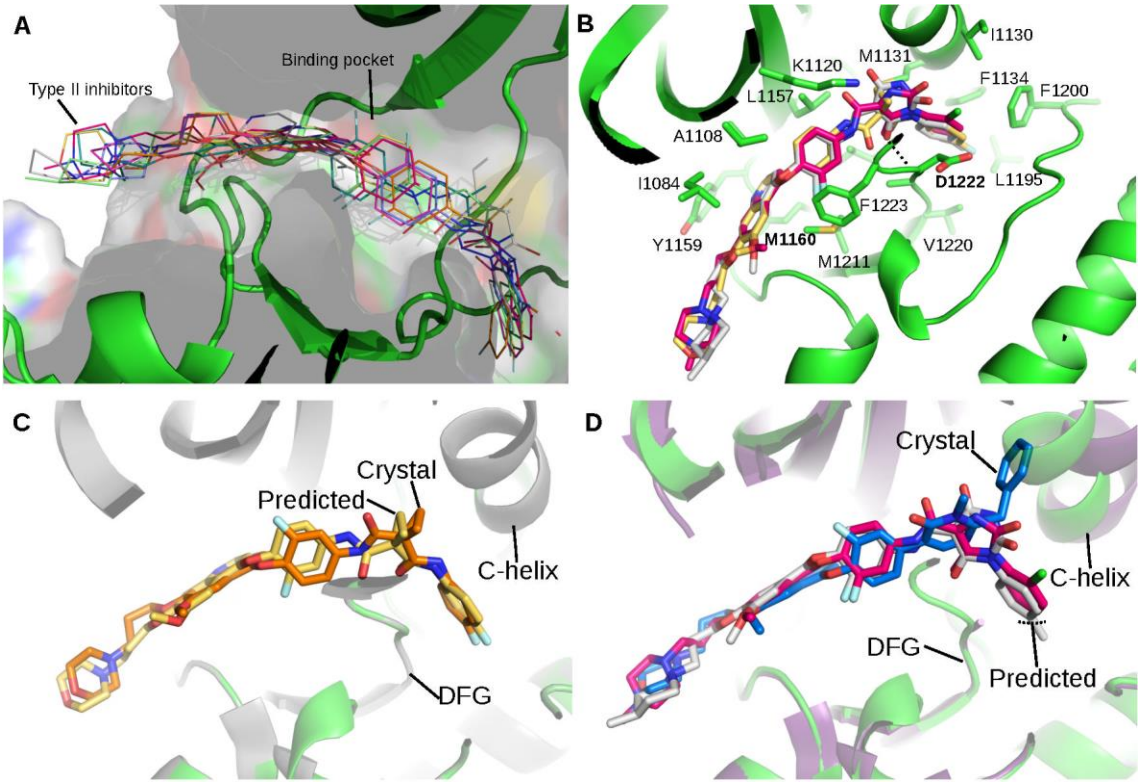

Fig. 7. Predicted binding modes of type II inhibitors to c-Met. A) Orientation of type II inhibitors in the ATP binding pocket. The inhibitors are shown in line representations, and the cross section of the binding pocket is fogged. B) Residues of the binding pocket interacting with the type II inhibitors. Residues that form hydrogen bonds with the ligands are labeled. Dashed lines represent hydrogen bonds at the interface. C–D) comparison of the binding mode of the compound determined by X-ray crystallography (pdb code: 3LQ8 in orange and 2RFN in blue) and predicted using docking of compounds **378** (yellow), **133** (gray) and **242** (magenta), respectively.